Visualization of electrostatic recognition by enzymes for their ligands and cofactors

Haruki Nakamura, Katsuichiro Komatsu*, Setsuko Nakagawa* and Hideaki Umeyama*

Department of Applied Physics, Faculty of Engineering, University of Tokyo, Bunkyo-ku, Tokyo 113, Japan
* School of Pharmaceutical Sciences, Kitasato University, Shirokane, Minato-ku, Tokyo 108, Japan

Electrostatic potentials for several enzymes and their guest molecules such as ligands and/or cofactors are individually calculated and illustrated as colour codes on their tertiary structures using a raster graphics technique. Two kinds of potential surface were illustrated on the molecular surface of the guest molecule. One is due to the host enzyme (H-on-G potential surface) and the other is due to the guest molecule itself (G-on-G potential surface). Remarkable mutual complementarities between the H-on-G and G-on-G potential surfaces were found in most cases. These give a semi-quantitative indication of the important role of electrostatic recognition in enzymes.

Keywords: raster graphics, electrostatic potential, enzymatic recognition

received 29 June 1984, accepted 29 September 1984

Recently, mechanisms of drug recognition by biomolecules have been analysed using an interactive graphic display of the vector scan type. Almost all the analyses have considered only steric or hydrophobic interaction between the host enzymes and the guest drugs or small molecules[1–3]. There have, however, been many descriptions which show the important role that electrostatic forces play in biomolecular interactions[4–9]. Only a few of these works[9,10], though, visualise and analyse the mechanism of electrostatic recognition by biomolecules.

One of us (H N) has previously proposed an approach to illustrating electrostatic molecular surfaces using a program named TERAS for a raster graphic display[11]. It forms an appropriate illustration of a molecule using a polygonal model, and the electrostatic potential at each constituent polygon is indicated by a corresponding colour code. Using TERAS, we introduce here a general graphic method, which visualizes how enzymes recognize their guest molecules such as substrates, inhibitors and/or cofactors electrostatically. We have found it a powerful tool in the analysis of methotrexate binding as an inhibitor to dihydrofolate reductase[12]. In the present paper, the method is described in detail, and its applications are shown for (1) flavodoxin (FXN)–flavin mononucleotide (FMN), (2) lactate dehydrogenase (LDH)–nicotinamide adenine dinucleotide (NAD^+), (3) glyceraldehyde phosphate dehydrogenase (GAPDH)–NAD^+–citrate and (4) lysozyme (LYZ)–trimer (MGM) of *N*-acetylmuramic acid (NAMB), *N*-acetylglucosamine (NAGC) and NAMD.

Method

Two kinds of electrostatic potential surface were calculated and illustrated. One is the host potential on the guest molecule (H-on-G potential surface: the electrostatic potential due to the host molecule on the van der Waals surface of the guest molecule), and the other is the guest potential on the guest molecule (G-on-G potential surface: the potential due to the guest molecule on the van der Waals surface of the guest molecule itself). Since the method used to generate the polygonal-surface model was described previously by Nakamura *et al*[11], only that used to calculate the potential is described below.

Firstly, tables of Mulliken net charges were made for the host enzymes and the guest molecules. For the host enzymes, the net charges were obtained from the charge table of the amino acid monomers made by Sheridan and Allen[13]. Lys, Arg, Glu, Asp, N-terminus and C-terminus residues were ionized, and His residues were ionized according to their environments. For the guest molecules, *ab initio* molecular orbital (MO) calculations with STO-3G basis sets were performed using the modified IMSPACK program[14]. All the atom positions except those of H-atoms were those given in the Brookhaven Protein Data Bank (PDB)[15]. Co-ordinates of H-atoms in the guest molecules were determined geometrically, considering possible hydrogen bonds to both the host and guest molecules. The procedure used to form the charge table in each of (1)–(4) is described in detail below, and all the Mulliken net charges obtained for the guest molecules are listed in the Appendix.

FXN–FMN

The atomic co-ordinates of the binary complex of FXN and oxidized FMN were obtained from 3FXN[16] in the PDB. Since FMN has too many molecular orbitals for a direct *ab initio* calculation, it was separated into two groups 1-deoxy-D-ribose-5-phosphate and lumiflavine.

The structure of oxidized FMN is shown in Figure 1(a). The positions of H-atoms in FMN were determined as follows: the co-ordinates of HO2* and HO4* were set so that they made hydrogen bonds to Ala55—O and Ser87—OG, respectively. HO3* was positioned so as to be oriented towards O4*. One H-atom in each of the C7M and C8M methyl groups was positioned in the plane of the isoalloxazine ring. H-atoms attached to N3, C6 and C9 of isoalloxazine were also positioned in the same plane. Co-ordinates of other H-atoms were determined geometrically, using the values of the bond angle, bond length and dihedral angle of methane. The net charge tables from MO calculations of the two groups in FMN were then joined together, and redundant values due to overlapping atoms were rejected. The total net charge of -2 was due to the phosphate group.

In FXN, there are no His residues and it was not necessary to consider their ionization.

LDH–NAD$^+$

The atomic co-ordinates of the complex LDH–NAD$^+$ were obtained from 3LDH[17] in the PDB. We assumed the same structure for NAD$^+$ as that in NAD–pyruvate in the PDB.

For the MO calculations, NAD$^+$ was separated into three groups: 5′-dehydroxymethyladenosine, methyl diphospho(5)1-dihydroxy ribose and 1-methylnicotinamide. The structure of NAD$^+$ is shown in Figure 1(b). The co-ordinates of HNO2*, HNO3*, HAO2* and HAO3* were determined so that the H-atoms were oriented towards Glu140-OE2, NO2*, Asp53-OD2 and Asp30-OD1, respectively. Nicotinamide and adenine H-atoms were placed in the plane of their respective aromatic rings with bond angles and bond lengths previously optimized for both molecules by *ab initio* MO calculations. Co-ordinates of other H-atoms were calculated geometrically as in the case of FXN–FMN. The total net charge of NAD$^+$ was -1.

The carboxamide groups of the Gln and Asn residues of the host enzyme LDH are ambiguous in 3LDH. A charge of -0.148 was assigned to both AE1 and AE2 for each Gln residue, and -0.150 to both AD1 and AD2 for each Asn residue, respectively. Residues 21, 82 and 104 are deficient, and were left untouched. The His 130 and 212 residues were ionized, since hydrogen bonds formed by the protonation of NE2 of the His residues lying above seemed possible. Calculations with His 95 ionized and unionized were considered since protonation of His 195 is associated with the reaction process of the enzyme[18]. Other His residues were not ionized.

GAPDH–NAD$^+$–Citrate

The atomic co-ordinates of the green subunit of GAPDH and those of NAD$^+$ are given in 1GPD[19] of the PDB. The co-ordinates of the bound citrate ion have been published for the green subunit[20].

NAD$^+$ was treated as three groups in the MO calculations in the same way as for LDH described above. The co-ordinates of HNO2*, HNO3*, HAO2* and HAO3* were determined so as to be oriented towards NO3*, Ser119-O, Asp32-OD2 and AO2*, respectively.

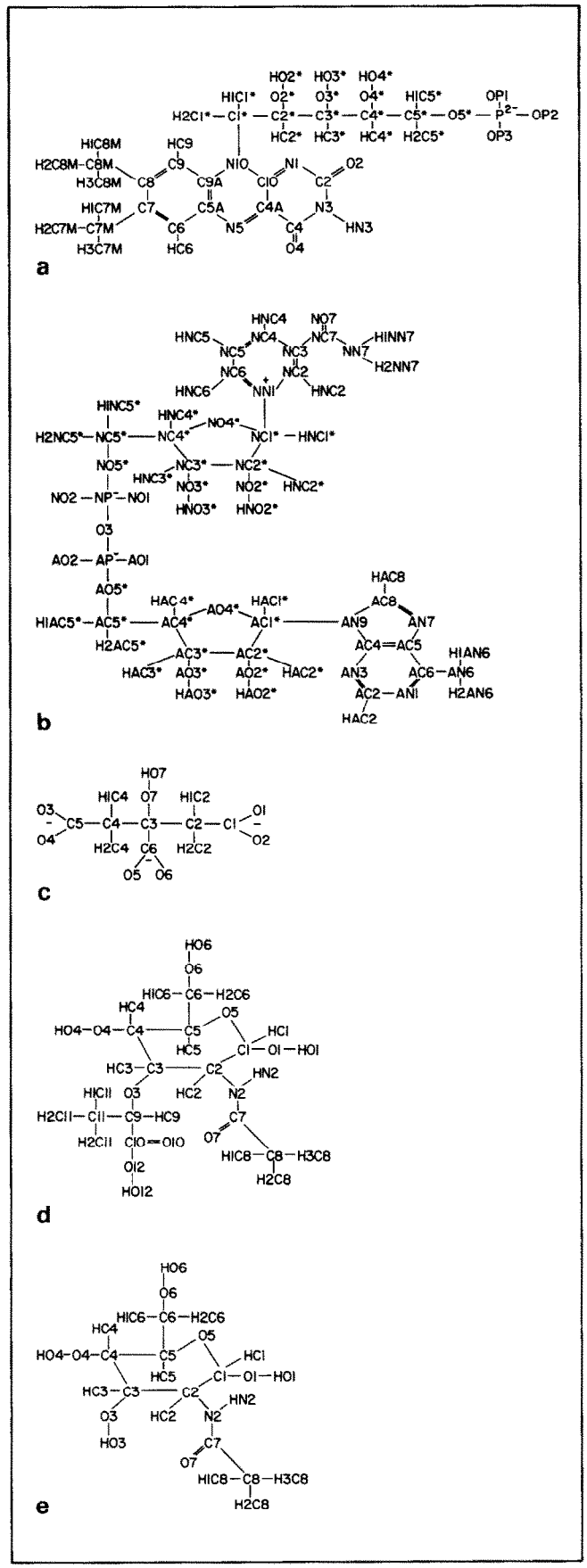

Figure 1. Covalent structures and atom numberings: (a) oxidized flavin mononucleotide (FMN), (b) nicotinamide adenine dinucleotide (NAD$^+$), (c) citrate, (d) N-acetylmuramic acid (NAM), and (e) N-acetylglucosamine (NAG)

Co-ordinates of other H-atoms were calculated as in LDH. The total net charge of the NAD^+ was -1.

The structure of the citrate ion is shown in Figure 1(c). The position of the H-atom attached to O7 of the citrate ion was determined so as to be oriented towards Cys149-SG. Other H-atoms in the citrate were determined geometrically.

In the host enzyme of GAPDH, the carboxamide groups of the Gln and Asn residues are also ambiguous. A charge of -0.148 was assigned to both AE1 and AE2 of each Gln residue, and -0.150 to both AD1 and AD2 of the Asn residues, except those of Asn313. From the relationship between the nicotinamide in NAD^+ and the carboxamide of Asn313, AD1 of Asn313 probably makes a hydrogen bond to NO7 of the NAD^+. AD1 and AD2 of Asn313 were therefore assigned as ND2 and OD1, respectively. His50, -100 and -162 were ionized. We considered ionization of Cys149 and His176 because (A) both are neutral groups and (B) Cys149-SG donates a proton to His176-NE2, to give SG^- and $NE2^+$. The process in (B) is required for the activated charge relay system in the catalytic reaction of the enzyme[21].

LYZ–MGM

The refined atomic co-ordinates of LYZ were obtained from 6LYZ[22] in the PDB. The co-ordinates of the bond sugar trimer MGM(B–C–D) are in 9LYZ[23] in the PDB.

The MGM was treated in the MO calculations as the three sugar monomers of NAMB, NAGC and NAMD. The structures of NAM and NAG are shown in Figures 1(d) and 1(e), respectively. The co-ordinates of NAMB-HO4, NAMB-HO6, NAGC-HO3, NAGC-HO6, NAMD-HO1 and NAMD-HO6 were determined so as to be oriented towards NAMB-O3, Asp101-OD2, NAMB-O5, NAGC-O5, Asp52-OD2 and Glu35-OE2, respectively. H-atoms were placed on the methyl carbons so as to minimize steric hindrance between the host lysozyme and MGM. Co-ordinates of other H-atoms were given geometrically. The MGM was overall neutral, since the NAM was not ionized.

According to the experimentally obtained pK value of 5.8 for His15 in the host lysozyme[24], interpolated values of its ionized and non-ionized partial charges were calculated at pH 7. Asp103 in 6LYZ was converted into Asn103. Two analyses of the catalytic reaction one with ionized Glu35 and the other with unionized Glu35 were considered. From the proposed scheme of the substrate reaction[25], Glu35 is not ionized in the ground state of the enzyme–substrate complex but is ionized in the transition state of the proton transfer.

To obtain the G-on-G potential surface, the electrostatic potential Ψ at a surface point of the guest molecule $\mathbf{r}_0$ was calculated following the classical formula:

$$\Psi(\mathbf{r}_0) = \sum_i \frac{q_i}{\epsilon_i |\vec{\mathbf{r}}_i - \mathbf{r}_0|} \qquad (1)$$

where the sum was taken only for the atoms of the guest molecule positioned at the $\mathbf{r}_i$ with partial charges q_i. For the H-on-G potential surface, the potential on the guest molecule was calculated from equation (1) using a summation which included atoms in the host enzyme and, in certain cases, the other ligands. In our previous paper[11], it was pointed out that there is a serious problem in estimating the dielectric constant ϵ_i in equation (1) for a strictly quantitative calculation of the electrostatic potentials. In the present study, we tentatively used two dielectric models with both constant and linear distance dependence. The two kinds of potential surface are very similar the difference being in the absolute potential values and in the more locally accentuated features in the model with linear distance dependence than those in the model with constant distance dependence. Since all the binding sites of the guest molecules examined in the present study are on the surface of the host enzymes, the screening effects of the solvent should be included to some extent. We show here the results for the dielectric model with linear distance dependence (from equation (2))

$$\epsilon_i = \begin{cases} 1 & (|\mathbf{r}_i - \mathbf{r}_0| \leqslant 1\text{A}) \\ |\mathbf{r}_i - \mathbf{r}_0| & (\text{otherwise}) \end{cases} \qquad (2)$$

RESULTS AND DISCUSSION

FXN–FMN

Colour plate 1(a) shows FMN bound to FXN and shows the main chain of the enzyme. The FMN binding site is the N-termini of parallel α-helices in the Rossmann fold, a characteristic of phosphate binding proteins[4,26,27].

Colour plate 1(b) shows the G-on-G potential surface of FMN as the guest molecule. The blue colour code indicates a relatively positive potential and the red code negative. The precise potential values are shown on the right hand side of the Plate. The G-on-G potential surface was negative throughout because of the phosphate group. Around the latter it was strongly negative but around the isoalloxazine ring it was weakly negative. The potential surface of HN3, HO2*, and HO4* were relatively more positive than that of their environments.

Conversely, the phosphate site potential has strongly positive values in the H-on-G potential surface shown in Colour plate 1(c), where FXN is the host enzyme. The mutual complementarity of the phosphate groups in the G-on-G and the H-on-G potential surfaces is a physically quantitative description of the hydrogen atom networks around the phosphate group listed in Table 1. The H-on-G potential surfaces around HN3, HO2*and HO4* are strongly negative. These have opposite signs in the corresponding G-on-G potential surfaces and these complementarities originate mainly from the hydrogen bonds in HN3 · · · Glu59-OE1, HO2* · · · Ala55-O and HO4* · · · Ser87-OG. We suggest that the complementarities indicate that many hydrogen bonds stabilise the binding of FMN, though there are no cationic residues near the phosphate binding site. However, the complementarity between the G-on-G and the H-on-G potential surfaces around the whole isoalloxazine ring is weak. It may indicate that electrostatic forces are not as important as hydrophobic effects in the recognition of this ring[16].

LDH–NAD^+

Colour plate 2(a) shows NAD^+ bound to LDH and the main chain of domain 1 of the enzyme. As a cofactor,

Table 1. Short contacts which may represent strong electrostatic interactions in the complex of oxidized FMN and FXN

FMN atom	FXN atom	Distance (Å)
OP1	Gly8-N	2.6
	Ser54-OG	2.8
OP2	Ser7-OG	2.6
	Thr12-OG1	2.8
	Thr12-N	3.0
OP3	Thr9-OG1	2.7
	Thr9-N	2.8
	Gly10-N	3.0
	Asn11-N	3.1
HO2*	Ala55-O	1.8
HO4*	Ser87-OG	2.1
O2	Gly89-N	2.9
	Trp90-N	3.4
	Gly91-N	3.1
HN3	Glu59-OE1	1.8
O4	Glu59-N	2.9

Table 2. Short contacts which may indicate strong electrostatic interactions between NAD^+ and LDH

NAD^+ atom	LDH atom	Distance (Å)
HAO2*	Asp53-OD2	1.8
HAO3*	Asp30-OD1	2.0
AO1	Arg101-NH1	2.8
NO1	Arg101-NH2	2.5
HNO2*	Glu140-OE2	2.5
HNO3*	Ala100-O	2.7
	Glu140-OE2	3.6
NO7	His195-NE2	3.4
	Lys250-NZ	4.3
H1NN7	His138-O	2.1
	Pro139-O	1.7
HNC2	His138-O	1.7
	Pro139-O	2.6
HNC4	O1B†	3.1

† O1B in the pyruvate, which is covalently bound to NAD in the original PDB data.

NAD^+ binds to the phosphate binding site of the Rossmann fold[26,27].

Colour plate 2(b) shows the G-on-G potential surface of NAD^+ as the guest molecule. The positive right region is the protonated nicotinamide which has a locally negative site at the oxygen of its carboxamide group. The intermediate pyrophosphate bridge is strongly negative and the adenine group shown on the left hand side of the colour plate has patches of weakly positive and negative potential.

In Colour plate 2(c), the H-on-G potential surface is shown, where NAD^+ and LDH are the guest and the host molecule, respectively. Here, His195 was not ionized. The potential surface of the phosphate group is strongly positive owing to the cation in Arg101, showing a reversal of the situation in the G-on-G potential surface in Colour plate 2(b).The potential in Colour plate 2(c) is strongly negative around NC2 and NN7 of the nicotinamide owing to the carbonyls of His138 and Pro139 also a direct contrast to the same area of the G-on-G potential surface. Moreover, there are further opposites in the G-on-G and H-on-G potential surfaces at —OH sites in the two sugar groups of HAO2*, HAO3*, HNO2* and HNO3*, owing to hydrogen bonds listed in Table 2. However, the H-on-G potential surface associated with the adenine ring has almost monotonically neutral values and no obvious complementarity with the corresponding section in the G-on-G surface was observed. The adenine site may be stabilized by hydrophobic effects rather than electrostatic forces[18].

When lactate binds to the binary complex of LDH–NAD^+, it has been proposed that His195 remains neutral in the reaction mechanism[18]. If His195 is protonated, the H-on-G potential surface around NC4 is very positive as shown in Colour plate 2(d) in contradiction to the positive values in the corresponding G-on-G potential surface in Colour plate 2(b). This excess of positive field cannot be compensated for by the substrate anion. It was tentatively put on the anion site of the pyruvate, the coordinates of which were given in the original x-ray data for the molecule covalently bound to LDH. It may be evidence that His195 is not protonated in the binary complex of LDH–NAD^+ before lactate binds to the complex.

GAPDH–NAD^+–Citrate

Colour plate 3(a) shows NAD^+ and citrate bound to GAPDH and shows the main chain of domain 1 of GAPDH. The citrate ion as a substrate analogue of the phosphate ion is positioned in the active centre region[20].

Colour plates 3(b) and 3(c) show G-on-G potential surfaces and Colour plates 3(d) and 3(e) are the corresponding H-on-G surfaces. Here NAD^+ is the guest molecule and GAPDH excluding citrate ion is the host molecule, Cys149-SG of which donates a proton to His176-NE2. The area representing the pyrophosphate group in the G-on-G potential surface is strongly negative (Colour plate 3(b)) and has a complementary relationship with the same area in the H-on-G potential surface which is strongly positive (Colour plate 3(d)). This effect is mainly due to Ilell-N and the side chains of Arg10 and Arg13. At the —OH sites in the sugar groups of HNO3*, HAO2* and HAO3*, distinct complementarities between the G-on-G (Colour plates 3(b) and 3(c)) and the H-on-G potential surfaces (Colour plates 3(d) and 3(e)) were observed, which are due to the hydrogen bonds listed in Table 3(a). The H-on-G potential surfaces around the adenine ring show values near to zero and have little complementarity with the corresponding G-on-G potential surfaces. Hydrophobic effects may be more essential than electrostatic interactions for recognition of the adenine ring[19].

One side of the nicotinamide ring (NC4, NC5 and NC6) is weakly negative in the H-on-G potential surface (Colour plate 3(e)), which indicates a protonated nicotinamide ring which has a strong positive field in the G-on-G potential surface (Colour plate 3(c)). When Cys149 and His176 were both neutral, the potential around NC4, NC5 and NC6 was positive as shown in Colour plate 3(f). This indicates that even without the substrate binding, the activated charge relay system with ionized Cys149 and His176[21] stabilizes the protonated nicotinamide ring. In the model system of the proton transfer in papain from a Cys to a His residue, it has been shown that the activated charge relay system is more stable than the neutral system without proton transfer, even when the substrate is absent[28]. A similar stabilizing mechanism may be working in the present system.

Table 3. Short contacts which may indicate strong electrostatic interactions in (a) NAD^+ and GAPDH and in (b) citrate and GAPDH–NAD^+

(a) NAD^+ atom	GAPDH atom	Distance (Å)
HAO2*	Asp32-OD2	1.9
HAO3*	Phe34-O	3.8
AO2	Arg13-NH1	4.9
NO1	Ile11-N	2.4
NO2	Arg10-NE	4.8
NO7	Asn313-ND2	3.8
H2NN7	Glu314-OE2	4.3
HNO3*	Ser119-O	2.0
NC5	Cys149-SG	4.3
	His176-NE2	6.9
(b) Citrate atom	GAPDH–NAD^+ atom	Distance (Å)
O1	Thr179-OG1	3.1
	Thr181-OG1	3.9
O2	Thr179-OG1	2.7
	Thr181-OG2	2.9
	Arg231-NH2	3.7
O4	Ser148-OG	3.0
	Thr208-OG1	3.3
O5	Arg231-NH1	3.0
O6	Arg231-NH1	3.0
	Arg231-NH2	3.1
HO7	Cys149-SG	3.0

Using the citrate analogue, the model of the ternary complex of the enzyme, coenzyme and the substrate can be visualized. Colour plate 3(g) shows the H-on-G potential surface, where NAD^+ is the guest molecule, and the binary complex of GAPDH and citrate is the host molecule. Here Cys149 and His176 make an activated charge relay system. There is an obvious potential decrease around the nicotinamide group in Colour plate 3(g) which contrasts more strongly with the G-on-G potential surface (Colour plate 3(c)) than that in Colour plate 3(e). Though the calculation used is approximate, it provides semi-quantitative evidence of the role of an activated charge relay system in stabilizing the NAD^+ binding.

On the other hand, Colour plates 3(h) and 3(i) show the G-on-G and H-on-G potential surfaces where citrate is the guest molecule and the complex of GAPDH and NAD^+ is the host molecule. The G-on-G potential is entirely negative probably because of the triply charged citrate ion[20]. Conversely, the H-on-G potential is completely positive. Especially, the top O6 site is strongly positive, owing to the contribution of Arg231-NH1 and -NH2. The potential around HO7 decreased owing to the anionic Cys149-SG. Colour plates 3(h) and 3(i) indicate the role of electrostatic forces in the activated charge relay system for substrate recognition of GAPDH–NAD^+.

LYZ–MGM

Colour plate 4(a) shows a view of MGM bound to LYZ and shows the main chain of the enzyme, viewed from outside the catalytic crevice.

Colour plates 4(b) and 4(c) show the G-on-G potential surfaces, viewed from outside and inside the crevice, respectively, with MGM as the guest molecule. Colour plates 4(d) and 4(e) are the H-on-G potential surfaces corresponding to Colour plates 4(b) and 4(c), respectively, where LYZ with undissociated Glu35 is the host molecule. The complementarity between Colour plates 4(b) and 4(d) is not as obvious as that between 4(c) and 4(e). In particular, the H-on-G potential surface (Colour plate 4(d)) of the carboxy group in NAMD oriented outwards into the solvent is not positive enough to be an exact opposite in sign to the potential surface in Colour plate 4(b). However, the edges of the H-on-G potential surface at NAMB-O10, NAMB-O7, NAGC-O6, NAGC-HN2 and NAMD-O6 were of distinctly opposite sign to those in Colour plate 4(b), because of the hydrogen networks indicated in Table 4.

On the other hand, Colour plate 4(e) shows a potential surface completely opposite to that in Colour plate 4(c), especialy at NAMB-HO12, NAMB-O7, NAMB-O10, NAMB-HO6, NAGC-O3, NAGC-O6, NAGC-O7, NAMD-O6 and NAMD-HO1. This indicates that the electrostatic interaction associated with the hydrogen bond networks[29] is essential in substrate binding to LYZ. The possible pairs of hydrogen bonds are listed in Table 4.

For the potential surfaces shown in Colour plates 4(d) and 4(e), Glu35 was not dissociated in the ground state of the catalytic reaction. From Phillips' scheme of the reaction[25], proton transfer from the carboxylate of Glu35 generates a carbonium ion at NAMD-C1 leaving Glu35 negatively charged. Colour plate 4(f) shows the H-on-G potential surface viewed from inside the crevice when Glu35 of the host LYZ was assumed to be ionized. It can be clearly seen that the potential around NAMD-C1 in Colour plate 4(f) is less than that in Colour plate 4(e). These are visualizations of the proposed mechanism of the reaction, in which the intermediate structure involved is electrostatically stabilized[30]. The correct intermediate may not have the same structure as the ground state, and many more quantitative calculations are necessary for a precise study of the catalytic reaction.

CORRELATION BETWEEN THE G-ON-G AND H-ON-G POTENTIAL SURFACES

As described above, it is certainly useful to illustrate both the G-on-G and H-on-G potential surfaces, but we propose here a more intensive approach to analyse their interrelation.

Table 4. Short contacts which may represent strong electrostatic interactions between MGM(B–C–D) and LYZ

MGM atom	LYZ atom	Distance (Å)
NAMB-O6	Asn103-ND2	4.2
NAMB-HO6	Asp101-OD2	3.9
NAMB-O7	Asn103-ND2	4.3
NAMB-O10	Asn103-ND2	2.2
NAMB-HO12	Asn103-OD1	3.4
NAGC-O3	Trp63-NE1	4.0
NAGC-O6	Trp62-NE1	3.1
NAGC-O7	Trp63-NE1	3.6
	Asn59-N	4.2
NAGC-HN2	Ala107-O	1.3
NAMD-O6	Val109-N	3.4
	Ala110-N	4.3
NAMD-HO6	Glu35-OE2	2.1
NAMD-O10	Asn46-ND2	3.0
NAMD-HO1	Asp52-OD2	4.1
NAMD-C1	Asp52-OD2	3.6
	Glu35-OE1	5.6
	Glu35-OE2	6.0

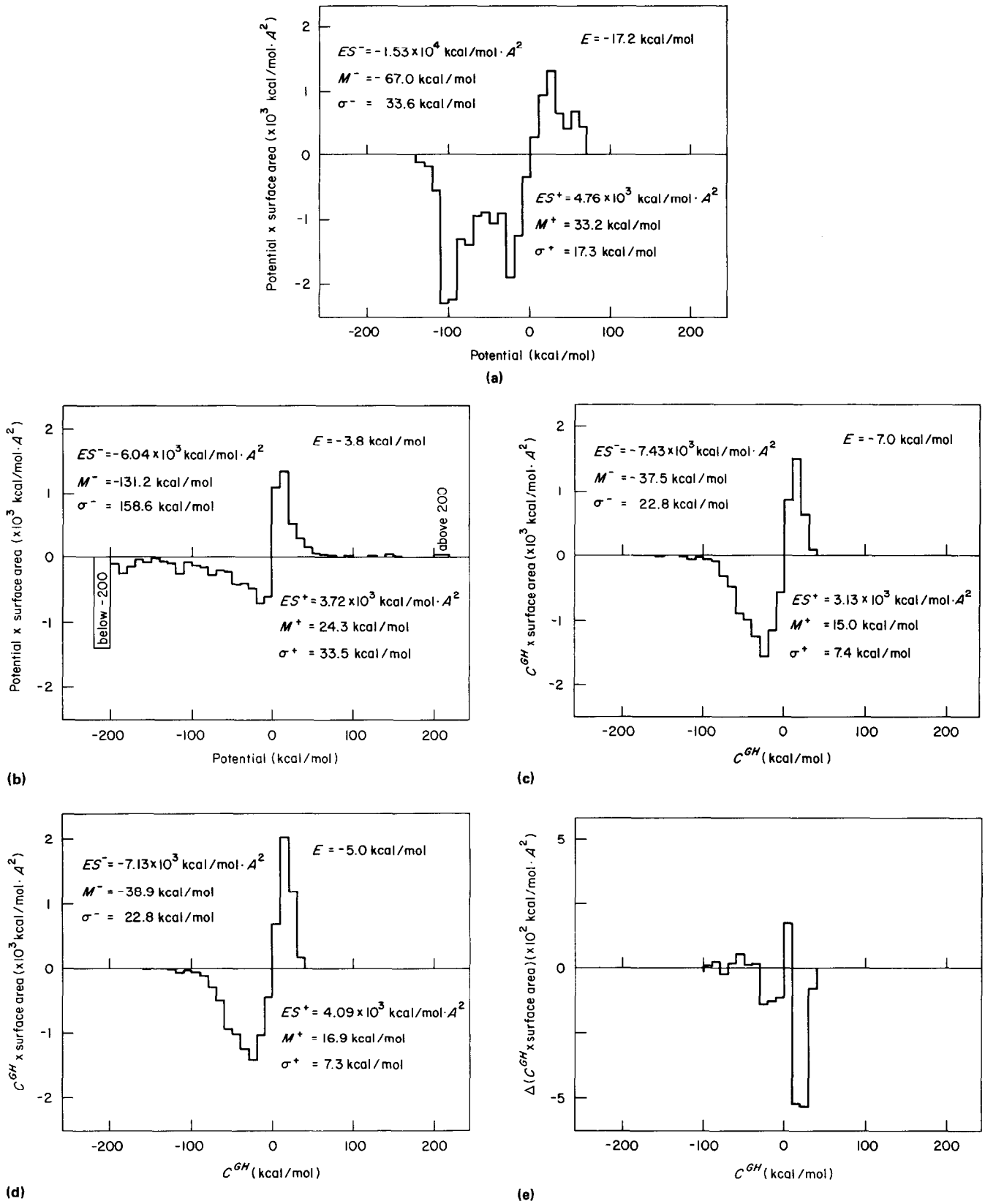

Figure 2. (a) Histogram corresponding to the G-on-G potential surface of NAD^+ in Colour plates 3(b) and 3(c). The abscissa is the potential value of each polygon making up the potential surface, and the ordinate is the product of the potential and the area of the polygon. The parameters are defined in the text; (b) histogram corresponding to the H-on-G potential surface shown in Colour plates 3(d) and 3(e), where the host molecule is GAPDH with an activated charge relay system including Cys149–SG^- and His176-$NE2^+$; (c) histogram corresponding to the G–H correlation surface shown in Colour plate 3(j), where the host GAPDH has an activated charge relay system; (d) histogram corresponding to the G–H correlation surface shown in Colour plate 3(k), where the host GAPDH has neutral Cys149 and His176; and (e) subtraction of the histogram in Figure 2(d) from that in Figure 2(c)

To quantitatively estimate an illustrated potential surface, we constructed the histogram shown in Figure 2(a), which corresponds to the G-on-G potential surface of NAD^+ shown in Colour plates 3(b) and 3(c). Here the abscissa is the potential of each polygon within the G-on-G potential surface, and the ordinate is the product of the potential and the area of the polygon. Parts of the histogram with both positive and negative potentials characterized by three parameters: $ES^{\pm}$, $M^{\pm}$ and $\sigma^{\pm}$, where $ES^{\pm}$ is the total sum of the product of the potential (e_i) and the area (s_i) of polygon i:

$$ES^{\pm} = \sum_i^{\pm} e_i s_i \tag{3}$$

and the superior symbol + or − indicates that the sum is taken only for polygons with positive or negative potential, respectively. Hereafter, the same rule applies; $M^{\pm}$ is the mean potential of each region with positive and negative potentials in the histogram:

$$M^{\pm} = \sum_i^{\pm} e_i^2 s_i / ES^{\pm} \tag{4}$$

and $\sigma^{\pm}$ is the standard deviation of each region with positive and negative potentials in the histogram:

$$\sigma^{\pm} = \left\{ \sum_i^{\pm} (e_i - M^{+})^2 e_i s_i / ES^{\pm} \right\}^{1/2} \tag{5}$$

There is another parameter E indicating the mean potential of the whole surface:

$$E = (ES^{+} + ES^{-})/(\text{total area of the whole surface}) \tag{6}$$

The values of these parameters are given in Figures 2(a–e).

Figure 2(b) shows the histogram corresponding to the H-on-G potential surface in Colour plates 3(d) and 3(e), constructed in the same way as Figure 2(a), where the host enzyme had an activated charge relay system with $Cys149^-$ and $His176^+$.

To characterize the complementarity between the guest and host molecules, a new parameter C_i^{GH} was introduced for each polygon i and defined as:

$$C_i^{GH} = \text{sign}\,(e_i^G e_i^H) \times |e_i^G e_i^H|^{1/2} \tag{7}$$

where e_i^G and e_i^H are the electrostatic potentials at the ith polygon in the G-on-G and H-on-G potential surfaces, respectively. C_i^{GH} is an energy term (kcal/mol). A large negative C_i^{GH}indicates a good complementarity and a large positive C_i^{GH}, a poor one. Figure 2(c) is a histogram showing the distribution of C_i^{GH} instead of e_i^G or e_i^H. Here, the parameter E reflects the degree of total complementarity.

Colour plate 3(j) illustrates a C_i^{GH} surface (hereafter called a 'G–H correlation surface'; a surface representing the correlation between the G-on-G and the H-on-G potential surfaces). It shows directly the complementarity between the guest and the host molecule. It can readily be seen that the complementarities of the pyrophosphate and nicotinamide groups are good, though not so good at the adenine ring, as already discussed above. Colour plate 3(k) shows the G–H correlation surface for the complementarities between Colour plate 3(c) and 3(f), where Cys149 and His176 of the host enzyme were neutral. The C_i^{GH} value at the nicotinamide was so positive in Colour plate 3(k), that we have worse complementarities in this case than those in Colour plate 3(j);. The histogram corresponding to Colour plate 3(k) is shown in Figure 2(d), and the difference between Figures 2(c) and 2(d) is shown in Figure 2(e). We found a lower E value in the activated charge relay system (Figure 2(c)) than that in the neutral system (Figure 2(d)). Figure 2(e) may explain why the former system is superior to the latter in enzymic recognition.

Colour plates 3(j) and 3(k) and the histograms in Figures 2(a–e), together with the parameters, seem to give a quantitative estimate of the degree of complementarity. However, we should point out here serious problems which include the approximate nature of the dielectric constant and the van der Waals surface in analysing enzymatic recognition using the histograms and parameters in Figures 2(a–e). They are that: (1) strictly speaking, C_i^{GH} does not correspond directly to the interaction energy between the guest and the host molecule. This parameter gives only the degree of the complementarity according to equation (7) between the pair of potentials on the surface of the molecule. (2) Equation (7) might not be the best definition for measuring the complementarity. In fact, some unrealistic results may occur if one of the pair of potential surfaces has a very strongly positive or negative value and the other has a value near zero. In such a case, the resulting positive or negative C_i^{GH} does not really indicate poor or good complementarity, respectively. There may be a more appropriate way to represent complementarities than equation (7). (3) The area of the van der Waals surface was introduced as a weight to average the histograms associated with the potential surfaces. But we may be able to use other potential surfaces which correspond to enzymatic recognition more directly than the van der Waals surfaces, such as a boundary surface between the guest and the host molecule at the interaction site.

Therefore, in the present study, it is dangerous to discuss and analyse quantitatively enzymatic recognition by use of only the histograms and parameters in Figures 2(a–e). To solve these problems, the characteristics of the histograms and the parameters and their correlations to physical quantities have to be established, such as the free energy decrease and the binding constant, by calculation for many cases. Moreover, we may have to introduce new parameters and representations, which correspond more directly to the physical quantities than the present histograms and parameters.

CONCLUSIONS

In conclusion, complementarity between G-on-G and H-on-G electrostatic potential surfaces was generally observed. That is, electrostatic forces work advantageously in most cases, and sometimes are essential in the binding of ligands and cofactors. The interacting sites utilising hydrogen bonds and salt bridges show distinct complementarities. The measurement of complementarity using introduced parameters which reflect the correlation between G-on-G and H-on-G potential surfaces was also effective.

On the other hand, several exceptions were observed, where the H-on-G potential surfaces did not give features opposite to those of the corresponding G-on-G potential surfaces.These were for the following cases, where (1) the potential surface faced the open solvent region, and did not directly interact with the host molecule but with the solvent molecules. Since we excluded solvent molecules from the host molecules in the present study, the interactions between the guest molecule and the solvent molecules were not visualized; (2) locally the hydrophobic effect was more essential than the electrostatic forces. This often occurred around the aromatic rings where both the G-on-G and H-on-G potential surfaces have values near zero. The poor complementaritiy may not lead to a large decrease in the binding free energy; (3) the dissociation of the ionizable residue was incorrectly assigned. In the present study, we assumed a neutral pH and the ionizations of only His residues were considered carefully. However, some ionizable residues, which have important roles in the enzymatic reactions, have specific pK values which indicate a neutral character. In such cases, the contradiction between the G-on-G and H-on-G potential surfaces were to be expected, when we did not consider the ionization state of these residues. From poor complementarities, we could ascertain the presence of significant residues, for example, those associated with the proton transfer mechanism. Appropriate assignment of the ionization of these residues then produces the desired complementarity; (4) there was a binding site for another ionic ligand in the neighbourhood of the guest molecule. In such cases, complementarity became better when the ionic ligand was included in the host molecule.

In the present study, only the H-on-G potential surfaces, based on co-ordinates from X-ray studies of the guest–host complex were calculated and visualized. That is, all the ligands and co-factors shown here have rather high affinities to the host enzymes. When this method is extended so as to be interactive, such that the positions of the potential surfaces can be moved and newly generated for new ligands, it may become much more useful to investigate recognition in biomolecules and to aid in design of new drugs or the modification of large biomolecules.

ACKNOWLEDGMENTS

The calculations and illustrations were performed at the Computer Centre, University of Tokyo. This work was partly supported by a Grant-in-Aid for Scientific Research from the Ministry of Education, Japan. The authors thank Professor N. Yasuoka, Institute for Protein Research, Osaka University, and Professor A. Wada, University of Tokyo, for their helpful comments and discussions.

REFERENCES

1 **Hansch, C, Li, R L, Blaney, J M and Langridge, R** *J. Med. Chem.* No 25 (1982) pp 777–784
2 **Li, R L, Hansch, C, Matthews, D A, Blaney, J M, Langridge, R, Delcamp, T J, Susten, S S and Freisheim, J H** *Quant. Struct.–Act. Relat.* No 1 (1982) pp 1–7
3 **Hansch, C, Hathaway, B A, Guo, Z R, Selassie,C D, Dietrich, S W, Blaney, J M, Langridge, R, Volz, K W and Kaufman, B T** *J. Med. Chem.* No 27 (1984) pp 129–143
4 **Hol, W G J, van Duijnen, P T and Berendsen, H J C** *Nature* No 273 (1978) pp 443–446
5 **Hol, W G J, Halie, L M and Sander, C** *Nature* No 294 (1981) pp 532–536
6 **Wada, A and Nakamura, H** *Nature* No 293 (1981) pp 757–758
7 **Umeyama, H, Nakagawa, S and Kudo, T** *J. Mol. Biol.* No 150 (1981) pp 409–421
8 **Matthew, J B, Weber, P C, Salemme, F R and Richards, F M** *Nature* No 301 (1983) pp 169–171
9 **Getzoff, E D, Tainer, J A, Weiner, P K, Kollman, P A, Richardson, J S and Richardson, D C** *Nature* No 306 (1983) pp 287–290
10 **Weiner, P K, Langridge, R, Blaney, J M, Schaefer, R and Kollman, P A** *Proc. Natl. Acad. Sci. USA* No 79 (1982) pp 3754–3758
11 **Nakamura, H, Kusunoki, M and Yasuoka, N** *J. Mol. Graph.* No 2 (1984) pp 14–17
12 **Komatsu, K, Nakamura, H, Nakagawa, S and Umeyama, H** *Chem. Pharm. Bull.* No 32 (1984) pp 3313–3316
13 **Sheridan, R P and Allen, L C** *J. Am. Chem. Soc.* No 103 (1981) pp 1544–1550 and its supplementary material
14 **Morokuma,K, Kato, S, Kitaura, K, Ohmine, I and Sakai, S** (1979) 'An *ab initio* program package consisting of Gaussian 70 and many other additional routines', unpublished work
15 **Bernstein, F C, Koetzle, T F, Williams, G J B, Meyer, E F, Jr, Brice, M D, Rodgers, J R, Kennard, O, Shimanouchi, T and Tasumi, M** *J. Mol. Biol.* No 112 (1977) pp 535–542
16 **Smith, W W, Burnett, R M, Darling, G D and Ludwig, M L** *J. Mol. Biol.* No 117 (1977) pp 195–225
17 **White, J L, Hackert, M L, Buehner, M, Adams, M J, Ford, G C, Lentz, P J, Jr, Smiley, I E, Steindel, S J and Rossmann, M G** *J. Mol. Biol.* No 102 (1976) pp 759–779
18 **Adams, M J, Buehner, M, Chandrasekhar, K, Ford, G C, Hackert, M L, Liljas, A, Rossmann, M G, Smiley, I E, Allison, W S, Everse, J, Kaplan, N O and Taylor, S S** *Proc. Natl. Acad. Sci. USA* No 70 (1973) pp 1968–1972
19 **Moras, D, Olsen, K W, Sabesan, M N, Buehner, M, Ford, G C and Rossmann, M G** *J. Biol. Chem.* No 250 (1975) pp 9137–9162
20 **Olsen, K W, Garavito, R M, Sabesan, M N and Rossmann, M G** *J. Mol. Biol.* No 107 (1976) pp 571–576
21 **Garavito, R M, Rossmann, M G, Argos, P and Eventoff, W** *Biochemistry* No 16 (1977) pp 5065–5071
22 **Diamond, R** *J. Mol. Biol.* No 82 (1974) pp 371-391
23 **Kelly, J A, Sielecki, A R, Sykes, B D, James, M N G and Phillips, D C** *Nature* No 282 (1979) pp 875–878
24 **Meadow, D H, Markley, J L, Cohen, J S and Jardetzky, O** *Proc. Natl. Acad. Sci. USA* No 58 (1967) pp 1307–1313
25 **Phillips, D C** *Sci. Am.* No 215 (1966) pp 78–90
26 **Rao, S T and Rossmann, M G** *J. Mol. Biol.* No 76 (1973) pp 241–256

27 Branden, C-I *Quart. Rev. Biophys.* No 13 (1980) pp 317–338
28 Umeyama, H and Nakagawa, S *Chem. Pharm. Bull.* No 29 (1981) pp 918–925
29 Imoto, T, Johnson, L N, North, A C T, Phillips, D C and Repley, J A *Enzymes* 3rd ed. No 7 (1972) pp 665–868
30 Warshel, A *Proc. Natl. Acad. Sci.* USA, No 75 (1978) pp 5250–5254

APPENDIX

Table A. Mulliken net atomic charges of oxidized FMN

Atom	Charge (e)	Atom	Charge (e)
N1	−0.3507	H2C7M	0.0692
C2	0.3788	H3C7M	0.0676
O2	−0.2765	H1C8M	0.0714
N3	−0.3948	H2C8M	0.0663
C4	0.3035	H3C8M	0.0715
O4	−0.2587	C2*	0.0755
C4A	0.0562	O2*	−0.3074
N5	−0.1900	C3*	0.0758
C5A	0.0512	O3*	−0.3390
C6	−0.0386	C4*	0.0455
C7	−0.0059	O4*	−0.3460
C7M	−0.1807	C5*	−0.0222
C8	0.0358	O5*	−0.4881
C8M	−0.1825	P	1.1882
C9	−0.0925	OP1	−0.8646
C9A	0.1240	OP2	−0.8618
N10	−0.2562	OP3	−0.8437
C10	0.2417	HC2*	0.0700
C1*	−0.0716	HO2*	0.1880
H1C1*	0.1190	HC3*	0.0300
H2C1*	0.0773	HO3*	0.2176
HN3	0.2260	HC4*	0.0420
HC6	0.0852	HO4*	0.2098
HC9	0.0682	H1C5*	0.0223
H1C7M	0.0677	H2C5*	0.0262

Table B. Mulliken net atomic charges of NAD^+ bound to LDH

Atom	Charge (e)	Atom	Charge (e)
AC4*	−0.0225	NO2	−0.8208
AO4*	−0.2351	NO5*	−0.4471
AC3*	0.0629	NC5*	0.0168
AO3*	−0.3072	NC4*	0.0708
AC2*	0.0438	NO4*	−0.2641
AO2*	−0.3151	NC3*	0.1158
AC1*	0.1736	NO3*	−0.3007
AN9	−0.2615	NC2*	0.0642
AC8	0.1298	NO2*	−0.3131
AN7	−0.2866	H1AC5*	0.0509
AC5	0.0073	H2AC5*	0.0661
AC6	0.2599	H1NC5*	0.0462
AN6	−0.4104	H2NC5*	0.0468
AN1	−0.3181	HNC4*	0.0685
AC2	0.1473	HNC3*	0.0711
AN3	−0.3134	HNO3*	0.2206
AC4	0.1827	HNC2*	0.0421
HAC1*	0.1091	HNO2*	0.2017
HAC2*	0.0770	NN1	−0.1787
HAC3*	0.0783	NC2	0.0977
HAO2*	0.2115	NC3	0.0051
HAO3*	0.2118	NC7	0.3106
HAC4*	0.0701	NO7	−0.2665
H1AN6	0.2259	NN7	−0.4340
H2AN6	0.2316	NC4	0.0892
HAC2	0.0790	NC5	−0.0584
HAC8	0.0999	NC6	0.1136
AP	1.2223	NC1*	−0.0569
AO1	−0.6817	HNC2	0.1230
AO2	−0.7422	HNC6	0.1552
AO5*	−0.4430	HNC5	0.1350
AC5*	−0.0654	HNC4	0.1739
O3	−0.6836	H1NN7	0.2263
NP	1.4622	H2NN7	0.2677
NO1	−0.7630	H1NC1*	0.1242

Table C. Mulliken net atomic charges of NAD^+ bound to GAPDH

Atom	Charge (e)	Atom	Charge (e)
AC4*	−0.0075	NO2	−0.7516
AO4*	−0.2575	NO5*	−0.4532
AC3*	0.0583	NC5*	−0.0063
AO3*	−0.3202	NC4*	0.0701
AC2*	0.0548	NO4*	−0.2331
AO2*	−0.3291	NC3*	0.0625
AC1*	0.1731	NO3*	−0.3259
AN9	−0.2683	NC2*	0.0621
AC8	0.1477	NO2*	−0.3228
AN7	−0.2758	H1AC5*	0.0879
AC5	0.0053	H2AC5*	0.0261
AC6	0.2647	H1NC5*	0.0378
AN6	−0.4103	H2NC5*	0.0894
AN1	−0.3192	HNC4*	0.0574
AC2	0.1541	HNC3*	0.0836
AN3	−0.3123	HNO3*	0.1988
AC4	0.1908	HNC2*	0.0961
HAC1*	0.0671	HNO2*	0.2016
HAC2*	0.0892	NN1	−0.1711
HAC3*	0.1134	NC2	0.1230
HAO2*	0.2082	NC3	0.0114
HAO3*	0.2105	NC7	0.3243
HAC4*	0.0628	NO7	−0.2333
H1AN6	0.2268	NN7	−0.4289
H2AN6	0.2277	NC4	0.0239
HAC2	0.0834	NC5	−0.0379
HAC8	0.0927	NC6	0.1231
AP	1.3683	NC1*	−0.0687
AO1	−0.7813	HNC2	0.1371
AO2	−0.7197	HNC6	0.1548
AO5*	−0.4746	HNC5	0.1417
AC5*	−0.0642	HNC4	0.1582
O3	−0.6952	H1NN7	0.2069
NP	1.3578	H2NN7	0.2455
NO1	−0.7431	H1NC1*	0.1311

Table D. Mulliken net atomic charges for Citrate ion

Atom	Charge (e)
C1	0.4202
O1	−0.5850
O2	−0.6486
C2	−0.1633
C3	0.1095
C4	−0.1495
C5	0.2012
O3	−0.5812
O4	−0.4971
C6	0.2096
O5	−0.5261
O6	−0.5506
O7	−0.3901
H1C2	−0.0414
H2C2	0.0057
H1C4	−0.0204
H2C4	0.0115
HO7	0.1956

Table E. Mulliken net atomic charges for NAMB-NAGC-NAMD

NAMB atom	Charge (e)	NAGC atom	Charge (e)	NAMD atom	Charge (e)
C1	0.1472	C1	0.1578	C1	0.1821
C2	0.0391	C2	0.0550	C2	0.0492
C3	0.0603	C3	0.0776	C3	0.0427
C4	0.0534	C4	0.0601	C4	0.1110
C5	0.0700	C5	0.0531	C5	0.0729
C6	0.0187	C6	0.0079	C6	0.0186
O3	−0.2934	O3	−0.3169	O1	−0.3144
O4	−0.3246	O4	−0.2703	O3	−0.2668
O5	−0.2473	O5	−0.2696	O4	−0.2999
O6	−0.3144	O6	−0.3253	O5	−0.2649
N2	−0.3754	N2	−0.3672	O6	−0.3105
C7	0.3013	C7	0.3021	N2	−0.4017
C8	−0.2062	C8	−0.2006	C7	0.2950
O7	−0.2833	O7	−0.2808	C8	−0.2074
C9	0.0315	HC1	0.1289	O7	−0.3021
C10	0.3323	HC2	0.0816	C9	0.0484
C11	−0.1874	HC3	0.0553	C10	0.3848
O10	−0.2879	HC4	0.0607	C11	−0.1831
O12	−0.3067	HC5	0.0646	O10	−0.3217
HC1	0.1182	H1C6	0.0694	O12	−0.2972
HC2	0.1025	H2C6	0.0623	HC1	0.0394
HC3	0.0569	HO3	0.2008	HC2	0.0947
HC4	0.0709	HO6	0.2064	HC3	0.1012
HC5	0.0568	HN2	0.1865	HC4	0.0495
H1C6	0.0577	H1C8	0.0821	HC5	0.0483
H2C6	0.0520	H2C8	0.0643	H1C6	0.0527
HC9	0.1205	H3C8	0.0731	H2C6	0.0504
HN2	0.1957			HC9	0.0713
HO4	0.1999			HN2	0.2316
HO6	0.1997			HO1	0.1984
HO12	0.2207			HO6	0.1991
H1C8	0.1001			HO12	0.2238
H2C8	0.0671			H1C8	0.0848
H3C8	0.0811			H2C8	0.0552
H1C11	0.0672			H3C8	0.0809
H2C11	0.0638			H1C11	0.0574
H3C11	0.0755			H2C11	0.0624
				H3C11	0.1115